

Random Fields and Random Anisotropies in the Mixed Ising-XY Magnet $\text{Fe}_x\text{Co}_{1-x}\text{TiO}_3$

Q. J. Harris, Q. Feng, Y. S. Lee, and R. J. Birgeneau

Department of Physics, Massachusetts Institute of Technology, Cambridge, Massachusetts 02139

A. Ito

Department of Physics, Faculty of Science, Ochanomizu University, Bunkyo-ku, Tokyo 112, Japan

(Received 5 August 1996)

We report a synchrotron x-ray scattering study of the phase transitions in the mixed Ising-XY magnets with quenched randomness: $\text{Fe}_x\text{Co}_{1-x}\text{TiO}_3$ as a function of x and, in the Ising regime, as a function of magnetic field. We observe at high resolution the loss of Ising order due either to the applied field on field cooling or to the ordering of the XY component after initial establishment of the Ising order on cooling. The latter is difficult to understand within our current picture of the random field Ising model. The XY phase has only short-range order due to random anisotropy effects. [S0031-9007(96)02155-2]

PACS numbers: 75.30.Kz, 75.40.Cx, 75.50.Lk, 78.70.Ck

In random magnets with competing interactions or fields, the two most basic questions are whether or not there exists a transition out of the high-temperature paramagnetic phase, and if there is a transition, whether it is to a state of conventional magnetic order or to a low-temperature disordered phase not present in uniform magnets [1]. A prototypical disordered system which has been the subject of much study, but where the above questions remain largely unanswered, is a mixed antiferromagnet with competing Ising and XY anisotropies [2–4]. In this case, both random anisotropy [5] and random field effects [6] are believed to be important. Further, as we shall show here, magnetoelastic effects also play an important role. By applying a magnetic field in the Ising phase, one may study the effects of externally generated random fields. Such mixed Ising-XY magnets thus represent a rich system for studies of the effects of random fields and random anisotropies.

In this note we report a high resolution synchrotron x-ray scattering study of the mixed Ising-XY magnetic system— $\text{Fe}_x\text{Co}_{1-x}\text{TiO}_3$ both in zero field and in an applied field. Both FeTiO_3 and CoTiO_3 have the same hexagonal structure [7], with the magnetic interactions between the neighboring Fe^{2+} (Co^{2+}) spins being ferromagnetic within the a - b planes, and antiferromagnetic between adjacent a - b planes [8]. Because of single ion anisotropy and/or anisotropic exchange, the easy axis of the Fe^{2+} spin (effective spin $S^{\text{Fe}} = 1$) is along the c axis (\parallel), while that of Co^{2+} ($S^{\text{Co}} = \frac{1}{2}$) is in the a - b plane (\perp). The Fe^{2+} and Co^{2+} spins thus have Ising and XY characters, respectively. Therefore, similar to $\text{Fe}_x\text{Co}_{1-x}\text{Cl}_2$ [2] and $\text{Fe}_x\text{Co}_{1-x}\text{Br}_2$ [3], this binary solid solution exhibits a tetracritical-like phase diagram with Ising, XY, and mixed phases. As emphasized by Wong *et al.* [2], there also exist random diagonal and off-diagonal coupling terms of the form $S_l(i)S_m(j)$ [$l, m = x, y(\perp)$ or $z(\parallel)$], which serve to generate random anisotropy and random field effects. Finally, in these systems there may be strong magnetoelastic coupling.

The phase behavior in $\text{Fe}_x\text{Co}_{1-x}\text{TiO}_3$ is thus the result of the collective effects of both fixed and random anisotropies and magnetoelastic coupling. This yields a rich phase diagram in the concentration (x) versus temperature (T) plane. Figure 1 is the phase diagram from Ref. [4] revised with the main results from this study: The low-temperature phase at low Fe^{2+} concentration (the area bounded by line AB and BD) is found to lack long-range order (LRO); instead, it is a \tilde{S}_\perp domain state; the line AB that separates the two disordered phases—paramagnet and \tilde{S}_\perp domain state—is an unusual *critical* line in the sense that the correlation length diverges on the line and yet there is no transition to LRO involved in

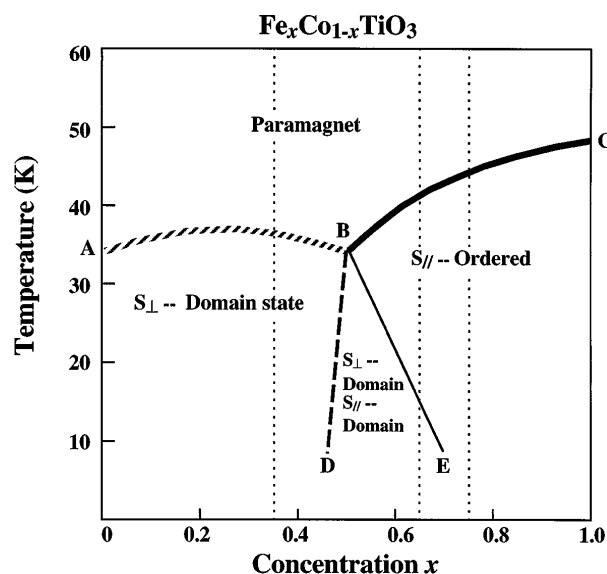


FIG. 1. The magnetic phase diagram of the crystalline binary compound $\text{Fe}_x\text{Co}_{1-x}\text{TiO}_3$ in the concentration (x) versus temperature (T) plane (from Ref. [4] revised with the main results from this work). The vertical dashed lines correspond to the actual concentrations studied.

this phase change. BC corresponds to a line of three-dimensional (3D) random exchange Ising transitions to LRO. With application of a field, $\text{Fe}_{0.75}\text{Co}_{0.25}\text{TiO}_3$ exhibits prototypical 3D random field Ising model (RFIM) behavior as observed previously in diluted antiferromagnets (as opposed to mixed magnets) in a magnetic field [6]. We observe in addition for the $x = 0.75$ sample a new magnetoelastic effect in which a uniform field induces a staggered charge density. Finally, in the mixed phase region, with decreasing temperature, Ising LRO is first established and then at lower temperatures when XY ordering occurs the Ising LRO is destroyed, that is, the Ising order is reentrant. The latter is difficult to understand within our current picture of the RFIM [6].

The experiments were carried out on the MIT-IBM beamline X20A at the National Synchrotron Light Source (NSLS) at Brookhaven National Laboratory. The white x-ray beam from the bending magnet was focused by a mirror and monochromatized by a pair of single bounce $\text{Ge}(111)$ crystals together with a $\text{Ge}(111)$ analyzer. The incident wavelength was set at $\lambda = 1.305 \text{ \AA}$. Excellent quality single crystals of $\text{Fe}_x\text{Co}_{1-x}\text{TiO}_3$ ($x = 0.35, 0.65,$ and 0.75), grown by the floating-zone method, with typical mosaicitities of 0.05° were used in the experiment. The sublattice magnetization measurements were carried out around the magnetic-superlattice positions $(0, 0, 4.5)$ and $(1, 1, 1.5)$. The magnetic x-ray intensities at $(0, 0, 4.5)$ and $(1, 1, 1.5)$ reciprocal-lattice positions in the spin-only approximation are proportional to $0.5|\tilde{S}_\perp|^2$ and $0.93|\tilde{S}_\parallel|^2 + 0.074|\tilde{S}_\perp|^2$, respectively.

We discuss first the behavior on the Ising side of the phase diagram. Detailed measurements were carried out on a sample of $\text{Fe}_{0.75}\text{Co}_{0.25}\text{TiO}_3$ both in zero field and for various applied fields. At zero field, a second order transition to LRO is observed at $T_N = 43.90(5) \text{ K}$. As shown in the top panel of Fig. 2, the intensity is well described by a simple power law $I \sim S_\parallel^2 \sim (1 - T/T_N)^{2\beta_\parallel}$ with $\beta_\parallel = 0.36(3)$ consistent with the theoretical value $\beta_\parallel = 0.35(1)$ for the 3D random exchange Ising model (REIM) [9]. Following the observation of Fishman and Aharony [10], the phase behavior of $\text{Fe}_{0.75}\text{Co}_{0.25}\text{TiO}_3$ in a uniform field should fall into the universality class of the 3D RFIM. The results for the correlation length on field cooling (FC) are shown in the bottom panel of Fig. 2. One observes a characteristic Lorentzian squared profile with a width κ_T which evolves continuously upon cooling, remaining nonzero as $T \rightarrow 0$, that is, the FC Ising transition is destroyed by the random field. On the other hand, after cooling to low temperatures in zero field and then applying a field (ZFC) the LRO is retained until the sample is heated above the metastability temperature $T_M(H)$. As may be seen in Fig. 2 the consequent order parameter curves are well described by the “*trompe l’oeil*” critical behavior model of Ref. [6] with $\beta_{\text{ZFC}} = 0.17(5)$, consistent with previous results. This behavior overall corresponds precisely to that observed in the

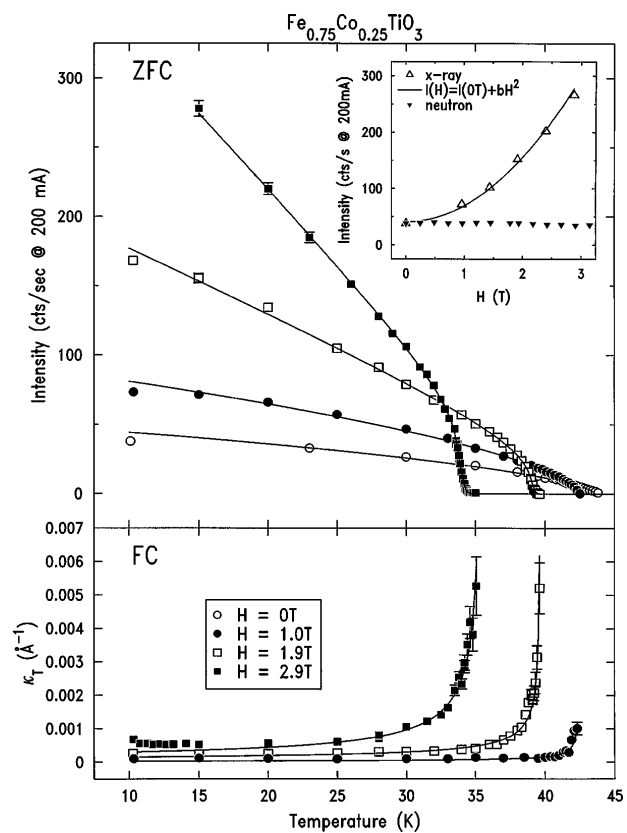


FIG. 2. RFIM behavior in $\text{Fe}_{0.75}\text{Co}_{0.25}\text{TiO}_3$ in a magnetic field. The upper panel shows the $(1, 1, 1.5)$ Bragg intensity after ZFC. The solid lines for $H \neq 0$ are the results of fits to the “*trompe l’oeil*” model of Ref. [6]. The $H = 0$ line is the result of a fit to a simple power law with $\beta_\parallel = 0.36(3)$. The inset shows the $(1, 1, 1.5)$ intensity for $T = 15 \text{ K}$ as a function of field for x rays and neutrons. The bottom panel shows the FC inverse correlation length κ_T for varied fields.

diluted antiferromagnets $\text{Fe}_x\text{Zn}_{1-x}\text{F}_2$ and $\text{Mn}_x\text{Zn}_{1-x}\text{F}_2$ thence confirming the universality of the phenomena and showing that such behavior is fundamental to the RFIM [6].

There is, however, one feature of the data in $\text{Fe}_{0.75}\text{Co}_{0.25}\text{TiO}_3$ shown in Fig. 2 which differs markedly from the behavior found in $\text{Fe}_x\text{Zn}_{1-x}\text{F}_2$ and $\text{Mn}_x\text{Zn}_{1-x}\text{F}_2$ [6]. Specifically, the ZFC x-ray intensity is observed to increase as H^2 . To probe this further, we have repeated the same measurements under identical conditions with neutron scattering techniques. The neutron and x-ray intensities at $(1, 1, 1.5)$ as functions of magnetic field for temperature $T = 15 \text{ K}$ are shown in the inset of Fig. 2; the intensities are normalized at zero field. As may be seen in Fig. 2, there is no significant field dependence of the neutron intensity; this rules out any explanation of the x-ray data based on an anomalous field-induced increase of the staggered Ising moment.

As an alternative explanation, we consider the possibility that the additional x-ray intensity at $(1, 1, 1.5)$ arises from an induced staggered lattice modulation. In order

to contribute to the x-ray scattering intensity at $(1, 1, 1.5)$, this charge density must have the same periodicity as the antiferromagnetic order. This modulation can be understood as originating from the coupling between the lattice and the magnetism via a coupling term of the form $\rho_s M_s M$, in which ρ_s is the staggered charge density, M_s is the staggered magnetic moment, and M is the uniform magnetization. A simple calculation yields $\rho_s \sim M_s M$. The x-ray scattering intensity at the reciprocal lattice point $(1, 1, 1.5)$ would now include both the magnetic contribution $I_M \sim M_s^2$, and a charge scattering contribution arising from this staggered charge density, $I_C \sim \rho_s^2 \sim (M_s M)^2 \sim M_s^2 H^2$ since $M \sim H$ at low fields. The scattering intensity at $(1, 1, 1.5)$ is then given by $I = I_M + I_C \sim M_s^2 + a M_s^2 H^2 = M_s^2(1 + aH^2)$, which is exactly the result displayed in the inset in Fig. 2. The discrepancy between x-ray and neutron measurements at the position $(1, 1, 1.5)$ may then be attributed to the fact that for neutrons the magnetic and nuclear scattering cross sections are comparable, whereas for x rays, charge scattering is intrinsically 6 orders of magnitude larger than magnetic scattering. This effect should occur in many different magnetic systems.

We now discuss the behavior in $\text{Fe}_{0.65}\text{Co}_{0.35}\text{TiO}_3$ which shows successive Ising and XY transitions with decreasing temperature. We show in Fig. 3 the temperature dependence of the integrated intensity, the peak intensity, the deconvolved in-plane transverse width κ_T , and the deconvolved longitudinal width κ_L of the magnetic reflection at the reciprocal-lattice position $(1, 1, 1.5)$. At a temperature $T_{\parallel}(x = 0.65) = 41.55(5)$ K, there is a sudden rise of the scattering intensity, indicating the onset of the ordering of the Ising magnetic component S_{\parallel} . For temperatures higher than ~ 17 K, this magnetic reflection is resolution limited, so that this phase has LRO. For T near $T_{\parallel}(x = 0.65)$, both the integrated and the peak intensity are well described by a simple power law, $[1 - T/T_{\parallel}(x = 0.65)]^{2\beta_{\parallel}}$ with $\beta_{\parallel} = 0.33(2)$, consistent with the theoretical result for the 3D REIM [9]. As the sample is cooled further down to below ~ 17 K, the magnetic reflection spectrum becomes broader with a corresponding decreasing peak intensity [Fig. 3(b)]. This indicates that below ~ 17 K, the magnetic structure is no longer long-range ordered. The line shape of the scattering profile is consistent with a Lorentzian-squared cross section which in three dimensions corresponds to pure exponential decay. Explicit deconvolution yields the results for the transverse and longitudinal widths κ_T and κ_L shown in Figs. 3(c) and 3(d), respectively. At $T = 10$ K, the in-plane domain size of the spin component S_{\parallel} is $\sim 2,000$ Å. This breakup into magnetic domains is clearly driven by the \vec{S}_{\perp} ordering at ~ 17 K. The latter is observed directly through the appearance of measurable magnetic scattering at $(0, 0, 4.5)$ below 17 K. Related effects have been observed by Endoh *et al.* [4] using neutrons, although there are quantitative discrepan-

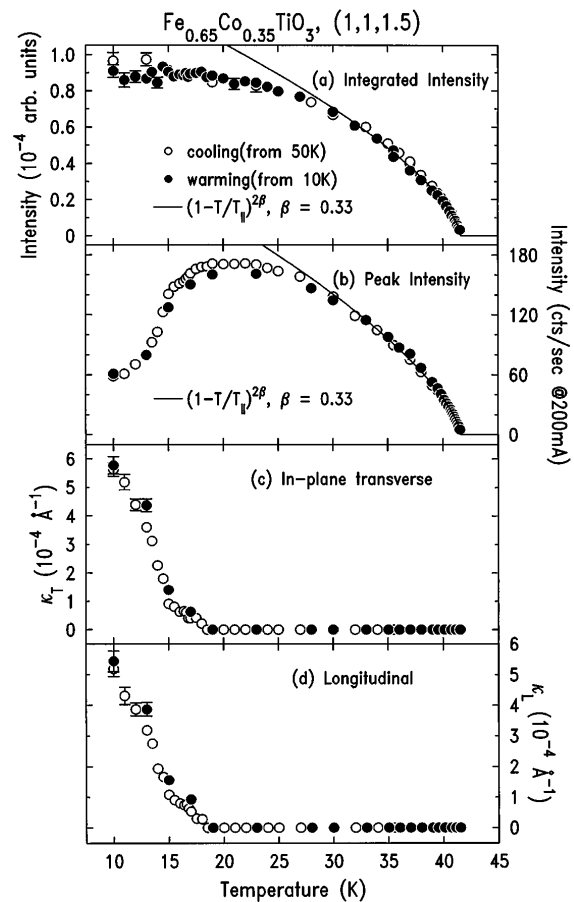


FIG. 3. Summary plots for the magnetic reflection $(1, 1, 1.5)$ for $\text{Fe}_{0.65}\text{Co}_{0.35}\text{TiO}_3$: (a) The integrated intensity as a function of temperature. (b) The peak intensity as a function of temperature. (c) The transverse width κ_T along the in-plane transverse direction as a function of temperature. (d) The longitudinal width κ_L along the longitudinal direction as a function of temperature. Here $S(\vec{q}) \sim (1 + [(q_L - q_L^0)/\kappa_L]^2 + [(q_T - q_T^0)/\kappa_T]^2 + [(q_V - q_V^0)/\kappa_V]^2)^{-1}$.

cies with our results presumably because the lower resolution neutron measurements probe the ordering over much shorter distance scales than x rays.

Before discussing the behavior below 17 K in the $x = 0.65$ sample, it is of value to present briefly the results in the sample with $x = 0.35$, which exhibits pure XY ordering. As in the samples which exhibit Ising order, one observes a sharp XY transition with $T_{\perp}(x = 0.35) = 36.89(3)$ K and power law behavior $I(0, 0, 4.5) \sim |\vec{S}_{\perp}|^2 \sim [1 - T/T_{\perp}(x = 0.35)]^{2\beta_{\perp}}$ for the order parameter with $\beta_{\perp} = 0.35(2)$ in quantitative agreement with the theoretical result $\beta_{xy} = 0.36$ for the 3D XY model [11]. However, there are two important differences in the behavior from that exhibited by the Ising samples. First, scans at the charge position $(1, 1, 0)$ reveal that there is a magnetoelastically driven distortion which breaks the in-plane hexagonal symmetry and causes crystallographic twinning. Second, the \vec{S}_{\perp} magnetic order is short range

with the domain size, which is infinite at T_{\perp} , decreasing progressively with decreasing temperature. The length scale, however, is quite large, typically of order 5000 Å. The structural peaks also are broadened, thus indicating that the short-range magnetic ordering causes the lattice to break up into structural domains. Thus the transition between the paramagnet and the \vec{S}_{\perp} -domain state (thick dashed line AB in Fig. 1) is unusual in the sense that the correlation length diverges along that line even though there is no low-temperature long-range ordered phase. This was implicit in Ref. [5] although these theories predict algebraic rather than the observed exponential decay below T_{\perp} . This apparent discrepancy may originate in the very large distance scales observed experimentally.

The breakup of the XY phases into magnetic and structural domains corresponds to our expectations for random anisotropy systems with strong magnetoelastic coupling. The most straightforward origin of the random anisotropy in $\text{Fe}_x\text{Co}_{1-x}\text{TiO}_3$ is the random nature of the mixture itself. Specifically, following Ref. [2], substitution of Co^{2+} ions with Fe^{2+} ions reduces the local symmetry of the crystal field acting on the Co^{2+} ions. This in turn induces random diagonal and off-diagonal exchange terms of the form $G_{lm}(ij)S_l(i)S_m(j)$ in the effective spin Hamiltonian. The \vec{S}_{\perp} -ordering transition thence should fall into the universality class of a 3D XY magnet with random anisotropy [5]. In the framework of the mean-field approximation, the anisotropy field $\vec{H}_A(i)$ at the i th spin is proportional to $[G_{xx}(ij) - G_{yy}(ij)]\langle|\vec{S}_{\perp}|\rangle$. This random anisotropy field is zero above the transition temperature $T_{\perp}(x = 0.35)$, but nonzero and increasing with decreasing temperature below $T_{\perp}(x = 0.35)$. This is consistent with the experimental findings discussed above. Random anisotropy effects originating from strains in the near-surface region probed by x rays presumably will also play a role.

We now return to a discussion of the re-entrant Ising behavior (Fig. 3) in the $x = 0.65$ sample. Both previous neutron studies on this sample and our own x-ray results show that the XY spin component S_{\perp} orders below 17 K. This causes a magnetoelastic distortion which in turn leads to twinning. This accounts for part of the transverse width κ_T observed at $(1, 1, 1.5)$, Fig. 3(c). In addition, following the discussion given above, off-diagonal random exchange terms of the form $G_{\perp\parallel}(ij)S_{\perp}(i)S_{\parallel}(j)$

will generate a random field $H_j^{\parallel} = G_{\perp\parallel}(ij)\langle S_{\perp}(i) \rangle$ acting on the Ising spin $S_{\parallel}(j)$. Naively, this S_{\perp} -driven random field effect would seem to explain the destruction of the Ising LRO below 17 K shown in Fig. 3(d). However, there is a serious caveat in this argument. Specifically, since the Ising LRO is well established above 17 K then the above process corresponds to the ZFC rather than FC procedure shown in Fig. 2 for the $x = 0.75$ sample in a field. Thus if the behavior corresponds to that observed in other RFIM systems, then the Ising random field created by the \vec{S}_{\perp} ordering should not have destroyed the Ising LRO. Apparently, therefore, the more complicated coupled Ising- XY nature of this system obviates the simple mean-field based analogy to the RFIM. Clearly a more sophisticated theory will be required to understand the rich physics exhibited by this system.

We would like to thank A. Aharony, M. Blume, L. D. Gibbs, J. P. Hill, D. A. Huse, and K. Katsumata for valuable discussions. We are especially grateful to M. Blume for providing us with the correct form for the $\rho_s M_s M$ coupling. The work at MIT was supported by the NSF under Grants No. DMR93-15715 and No. DMR94-00334.

-
- [1] Y. Imry and S-K Ma, Phys. Rev. Lett. **35**, 1399 (1975).
 - [2] P. Wong *et al.*, Phys. Rev. B **27**, 428 (1983).
 - [3] K. Katsumata *et al.*, Phys. Rev. B **30**, 1377 (1984).
 - [4] A. Ito *et al.*, J. Phys. Soc. Jpn. **51**, 3173 (1982); Y. Endoh, *ibid.* **55**, 240 (1986).
 - [5] A. Aharony and E. Pytte, Phys. Rev. Lett. **45**, 1583 (1980); J. Villain and J.F. Fernandez, Z. Phys. B **54**, 139 (1984); R. Fisch, Phys. Rev. B **51**, 11 507 (1995).
 - [6] J.P. Hill *et al.*, Phys. Rev. Lett. **70**, 3655 (1993); R.J. Birgeneau *et al.*, Phys. Rev. Lett. **75**, 1198 (1995), and references therein.
 - [7] R.W.G. Wyckoff, *Crystal Structures* (Interscience Publishers, New York, 1963).
 - [8] G. Shirane *et al.*, J. Phys. Chem. Solids **10**, 35 (1959); R.E. Newnham *et al.*, Acta Crystallogr. **17**, 240 (1964).
 - [9] K.E. Newman and E.K. Riedel, Phys. Rev. B **25**, 264 (1982); G. Jug, *ibid.* **27**, 609 (1983).
 - [10] S. Fishman and A. Aharony, J. Phys. C **12**, L729 (1979).
 - [11] J.C. Le Guillon and J. Zinn-Justin, Phys. Rev. B **21**, 3976 (1980).